Asian Journal of Chemistry; Vol. 25, No. 9 (2013), 4948-4952

ASIAN JOURNAL OF CHEMISTRY

http://dx.doi.org/10.14233/ajchem.2013.14154

Experiment and Modeling of Water Vapour Decomposition on $ZrNi_5$ Alloy

YONG YAO*, DELI LUO, ZHIYONG HUANG and JIANGFENG SONG

Science and Technology on Surface Physics and Chemistry Laboratory, Mianyang 621907, P.R. China

*Corresponding author: Fax: +86 816 3620285; Tel: +86 816 3620285; E-mail: yaoyongcaep@sina.com

(*Received*: 6 June 2012; *Accepted*: 11 March 2013) AJC-13110

In order to simulate tritium recovery from tritiated water by hot metal bed.$ZrNi_5$ powder was used to decompose water vapour in inert gas argon. Kinetics of the reaction was studied by thermogravimetric analyzer, the reaction mechanism at 723 K could be described by first-order chemical reaction. One-dimensional quasi-homogenous model was built to predict the breakthrough performance of the fixed bed reactor, the model integrated with kinetics parameter was solved by comsol multiphysics. The predicted breakthrough curves were compared with experiment data, it was shown that the modeling results agree well with experiment.

Key Words: $ZrNi_5$, Water decomposition, Kinetics, One-dimensional quasi-homogenous model.

INTRODUCTION

Tritiated water (HTO) production is unavoidable in tritium processing plant. It always formed by the isotope exchange between tritium and water vapour permeated in glove box[1]. Tritiated water will also be produced in air detritiation system by catalytic oxidation in the event of tritium release[2]. Tritiated water is *ca.* 30000 times more radio-toxic for human bodies than tritium[3]; tritium in the chemical form of hydrogen molecules is by far the safest, therefore the processing and storage of tritiated water in liquid must be avoided if possible[4,5]. Furthermore, tritiated water could not be utilized directly, it must be transformed to elemental tritium. Hence extracting tritium from tritiated water is important for both tritium recovery and environment security.

Tritiated water reduction on metal getters offers a simple and cost-effective solution to recovery tritium and reduce tritium emission. In this approach, tritiated water vapour is converted to tritium by redox reaction[6]. In order to reduce the tritium permeation at high temperature, the reducing bed should work at relative low temperature and the material should have small hydrogen inventory[7]. ZrMnFe (trade mark st909) is the most widely used material, but the price is too high-around $4000-$4500($US)/kg[8]. It is necessary to find a less expensive material with the similar property. $ZrNi_5$ may be a good candidate, for it doesn't hydrogenate unless at very high pressure and has a little hydrogen inventory[9,10] and the attracting advantage is the low price, only 1/30 to st909.

On the other hand, it is necessary to establish a model that could describe the bed performance subjected to different operation conditions. Once the model has been validated, it can minimize the number of experiments associated with new operating conditions, therefore decrease additional costs and radioactivity harm. However, there are far fewer applications of fixed-bed modeling to predict the breakthrough performance of water decomposition.

In this work, H_2O was used to substitute tritiated water because that hydrogen isotopes have similar chemical property and H_2O has no radioactivity. The objective of this study is to investigate the kinetics of water decomposition by $ZrNi_5$ and establish a mathematic model integrated with kinetics data to predict the fixed bed performance for water decomposition.

EXPERIMENTAL

$ZrNi_5$ alloy powders (granularity 400-500 meshes) was purchased from JinZhou Metal Material Institute. Certified gas mixture of Ar with trace H_2 (10000, 6000 and 3000 ppm) was purchased from Chinese Academy of Measurement Technology.

Thermogravimetric kinetics: The schematic diagram of the thermogravimetric experiment arrangement is shown in Fig. 1. ZCT-TGA with the sensitivity of detecting weight changes on the order of 1 μg was used in the experiments. 5 N Ar was first introduced into the TG reactor chamber, sample was heated to the reaction temperature with the protecting of argon. Then H_2O/Ar mixture was sent into TGA, the mass variation of sample and reaction time was recorded by computer and the conversion rate was described by the sample mass increased divided by the maxium mass increment. Quantitative

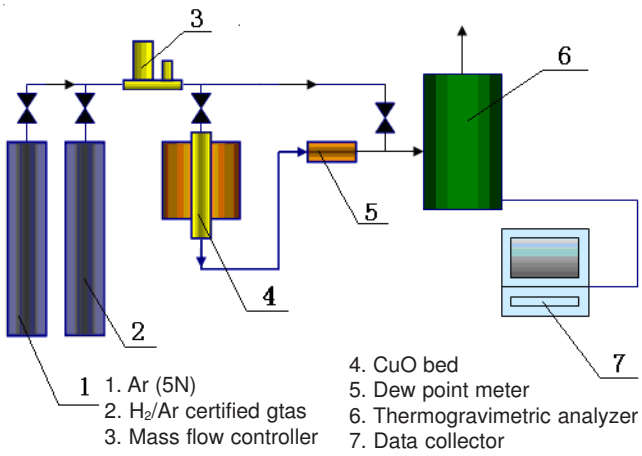

Fig. 1. Schematic diagram of thermogravimetric experiment

water was produced by the reaction: $H_2 + CuO = Cu + H_2O$ in CuO bed, the bed temperature was keeping at 773 K and CuO was overloading to ensure all hydrogen molecule could be oxidized to water. Water concentration was monitored by dew point meter (MichellCermax). Pre-experiment was carried out first to eliminate the influence of external diffusion by increasing the flow velocity and scattering sample uniformly on platinum crucible.

Water decomposition in fixed bed reactor: Water decomposition in a continuous-flow system was carried out in a fixed bed reactor(stainless steel tube with inner diameter 8.5 mm, column length 400 mm). The experiment setup of the reactor is shown in Fig. 2. $ZrNi_5$ powder was diluted by SiO_2 powder (140-230 meshes) with the mass ratio 1:4, the adding of SiO_2 was aimed to distribute $ZrNi_5$ powder uniformly in the reactor to diminish flow short-circuit and agglomeration. The reactant was underlain by glass wool to improve the flow distribution.

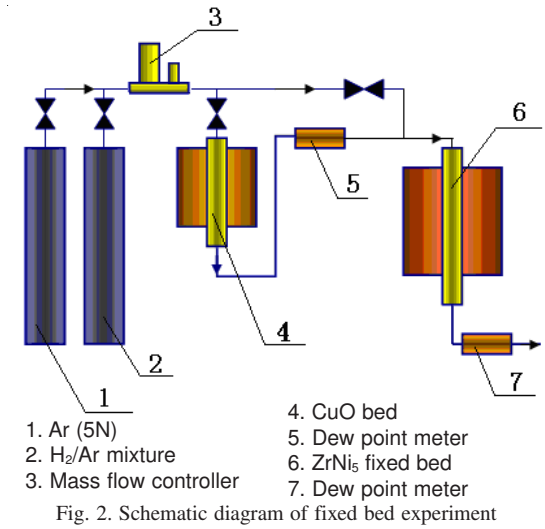

Fig. 2. Schematic diagram of fixed bed experiment

Before each experiment, the sample was heated to reaction temperature in 5 N Ar. Quantitative water was produced by the same way in TG experiment. The breakthrough curve was obtained by recording outlet water concentration *versus* time. The total amount of water decomposed (m_{total}) was represented by the area above the breakthrough curve (c *versus* t) through numerical integration[11]. The amount of water vapour decomposed at breakthrough point was calculated from following equation:

$$m_{break} = c_0 \times u \times t_b \quad (1)$$

where c_0 is water initial concentration, u is superficial velocity, t_b is time when the outlet water concentration rise to 1 % of initial gas. The maximum amount of water decomposed m_{max} was calculated from alloy maximum mass increment caused by oxygen absorption, where oxygen is equimolar amount to H_2O.

Modeling method: The system under consideration is an fixed-bed. The following assumptions are made: The fixed bed is isothermal, gas is plus flow and velocity is constant, axial dispersion is negligible for alloy powder size is small compared with the diameter and length of the bed, the reaction is irreversible. One-dimensional quasi-homogenous model of the fixed-bed reactor is based on the conservation equation[12,13]:

$$\frac{\partial c}{\partial t} = -u\frac{\partial c}{\partial z} - \left(\frac{\rho_b}{\varepsilon b}\right)\frac{\partial x}{\partial t} \quad (2)$$

where ρ_b, ε, u and b are $ZrNi_5$ powder density in fixed bed, the void fraction of bed, the interstitial velocity of gas and stoichiometric coefficient of chemical reaction, respectively. The operation time and the distance from the inlet of the gas are shown by t and z, respectively. c and x are the water concentration in Ar and alloy conversion rate, respectively. ∂x/∂t can be obtained by thermalgravimetric kinetics data.

The model equation obeys the following initial condition and boundary condition:

$$c = 0 (t = 0, 0 \le z \le L) \quad (3)$$

$$\frac{\partial c}{\partial z} = 0 (z = L) \quad (4)$$

$$u \times c\big|_{z=0^-} = \left(u \times c - D_L \frac{\partial c}{\partial z}\right)_{z=0^+} (z = 0) \quad (5)$$

eqn. 2 was solved by Comsol Multyphysics with PDE modes.

RESULTS AND DISCUSSION

Characterization of material: Fig. 3 shows the XRD spectrum. The alloy mainly consists of $ZrNi_5$ phase, with trace ZrO_2 and Ni before reaction. After reaction, the $ZrNi_5$ phase disappeared and the phase is comprised of ZrO_2 and Ni. This indicates that Zr is effective element to split H_2O,while Ni couldn't split H_2O and remained in elemental form. The process is similar to the reaction of water and ZrNi alloy[14]. The reaction equation could be speculated as following:

$$ZrNi_5 + 2H_2O(g) = ZrO_2 + 5Ni + 2H_2(g) \quad (6)$$

The sample mass increment is 8.3 % calculated from eqn. 6, which is equal to the maximum increment in experiment.

Thermogravimetric kinetics: Three temperatures (673, 723 and 773 K) was selected for decomposition reaction with water concentration 10^4 ppm. Fig. 4 shows alloy conversion rate with reaction time. It was found the higher temperature the faster reaction rate, the time for complete conversion was

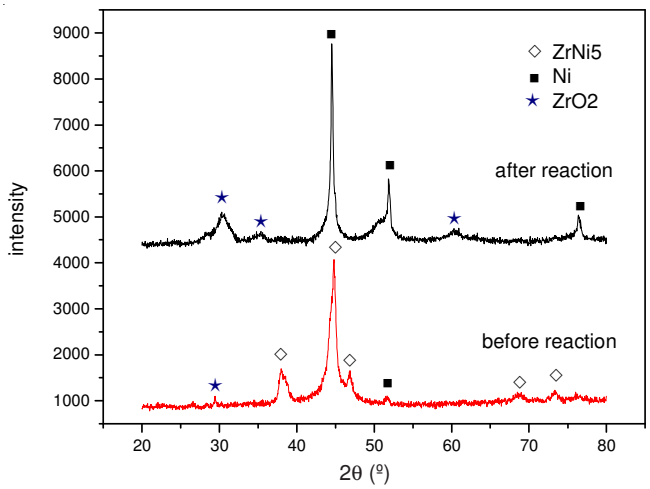

Fig. 3. XRD spectrum before and after reaction

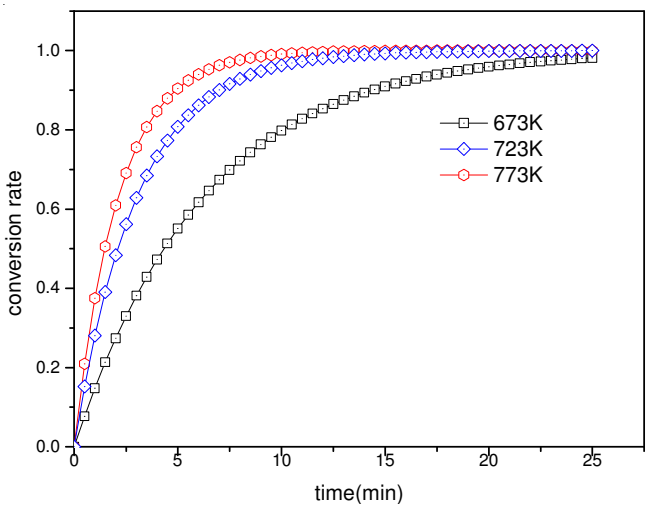

Fig. 4. Effect of temperature on reaction rate

more than 25 min for 673 k, but only 12 min for 723 K and 10 min for 773 K. The reaction rate at 723 K is close to that at 773 K, but hydrogen permeation is only 3/8 of that at 773 K[15], lower temperature is crucial to reduce hydrogen permeation in practical tritiated water treatment. 723 K seems a suitable temperature both for high reaction rate and low hydrogen permeation. 723 K was selected in the following kinetics experiment.

The reaction was carried out with three water concentration (10000, 6000 and 3000 ppm) at 723 K. The result is shown in Fig. 5, the time for complete reaction was 12 min for 10000 ppm, 18 min for 6000 ppm and more than 30 min for 3000 ppm. The higher reaction rate resulted from higher collision frequency between water molecule and alloy particle surface at higher water concentration. Some mechanism equations (Table-1) were used to elaborate the reaction process. Data with 10000 ppm was took into the four equations, the linearity of G(x)-t is shown in Fig. 6 and square of relative correlation (R^2) shown in Table-1. From the results it could seen that the chemical reaction of first order is the best to describe the mechanism, with R^2 equal to 0.99, so eqn. 10 is the most possible model. In order to ensure this, the data with the other two concentration was processed by the same way, the result is shown in Fig. 7, the linearity is very good too. The slope is known as apparent rate constant, K. K is 0.33, 0.20 and 0.09

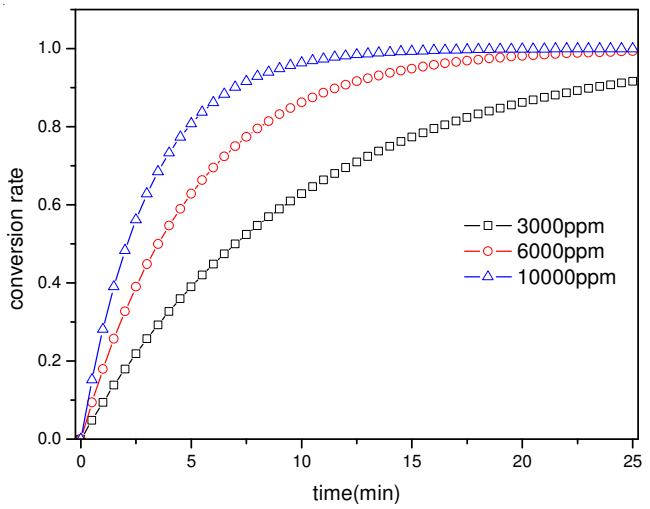

Fig. 5. Effect of water concentration on reaction rate

TABLE-1
CLASSICAL EQUATIONS OF SOLID-STATE PROCESS[16]

Process	G(x)		R^2
Nucleation with three dimensional growth	$3[-\ln(1-x)]^{1/3}$	(7)	0.843
Nucleation with two dimensional growth	$2[-\ln(1-x)]^{1/2}$	(8)	0.939
Two dimensional diffusion	$(1-x)\ln(1-x)+x$	(9)	0.931
Chemical reaction of first order	$-\ln(1-x)$	(10)	0.99

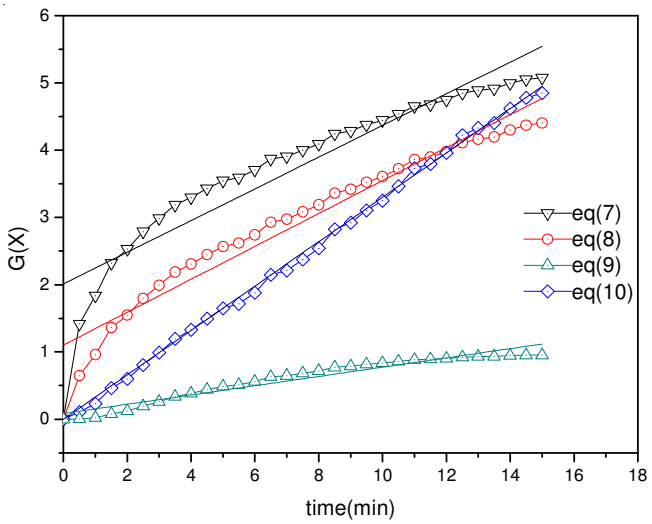

Fig. 6. Fitting of experimental data with mechanism equation

min^{-1} for 10000, 6000 and 3000 ppm, respectively. The relation of K and water concentration is shown in Fig. 8, it was found that K is proportional to concentration. The slope is described as $k' = 3.33 \times 10^{-5}$ ppm^{-1}, where k' is the alloy intrinsic properties at 723 K. Combining k' and the differential form of the G(x) of eqn. 10, the reaction rate with water concentration could be written as following:

$$\frac{dx}{dt} = K(1-x) = k'c(1-x) \quad (11)$$

The breakthrough curve could be obtained by solving differential eqn. 2 and 11.

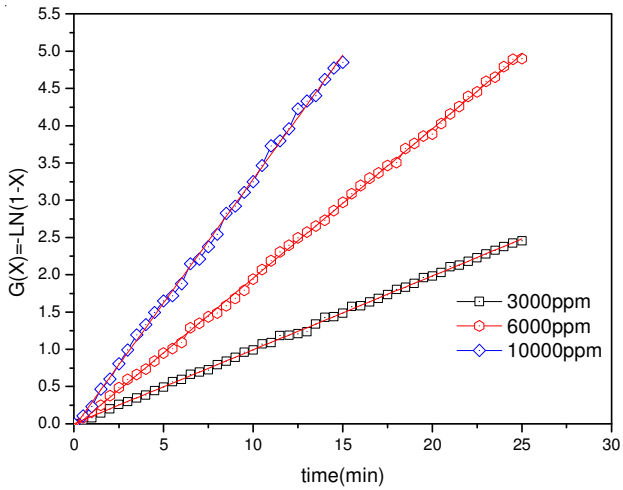

Fig. 7. Mechanics curve of different water concentration

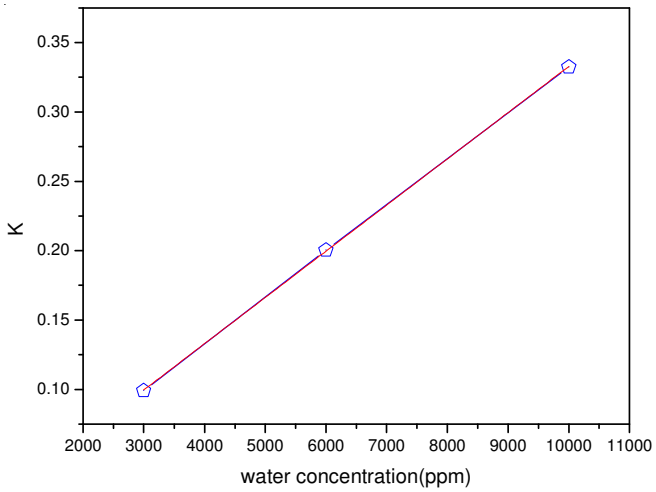

Fig. 8. Rate constant *versus* water concentration

Fixed bed reactor performance: Water concentration, flow rate and alloy mass are considered in the column experiment. The parameters are shown in Table-2.

Effect of water concentration: The effect of initial water concentration, varying from 3000-10000 ppm, at flow rate of 175 mL/min and alloy mass of 0.5 g is shown in Table-2 and Fig. 9. By increasing the feeding concentration, the volume of gas treated before breakthrough point was considerably reduced. This is due to the fact that the fixed bed is easily saturated at higher concentrations; thereby the breakthrough time is reached faster. The m_{break} and m_{total} didn't changed obviously with different water concentration.

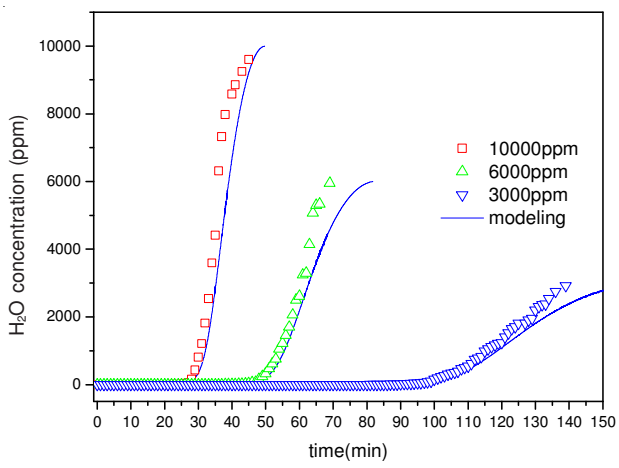

Fig. 9. Effect of water concentration on breakthrough curve

Effect of flow rate: The effect of feed flow rate on water decomposition by $ZrNi_5$ was investigated by varying the flow rate from 100-250 mL/min with fixed alloy mass and water concentration. The results are presented in Fig. 10 and Table-2. It was found that increasing the gas velocity was associated with decreasing in breakthrough time. Furthermore, the amount of water decomposed also decreased, m_{break}/m_{max} decreased from 84.6 to 61.1 %, m_{total}/m_{max} decreased from 96.6 to 90.7 %, respectively. The decrease is due to the insufficient residence time of the water vapour within the bed at higher flow rate, higher velocity leads to weaker interaction between alloy powders surface and water molecules resulting in less absorption. So the lower flow rate contributes to higher ratio of water decomposition and alloy utilization.

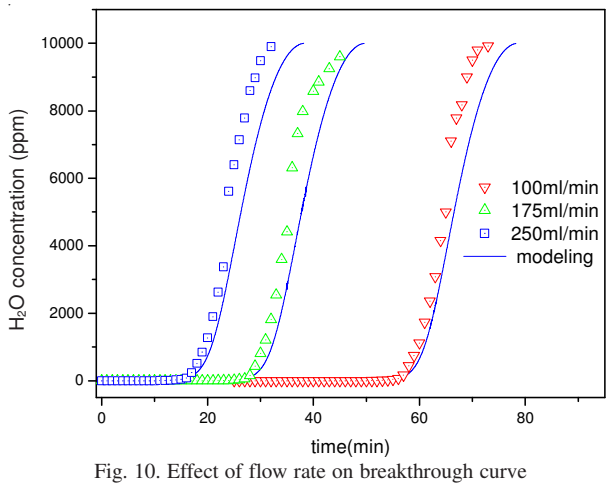

Fig. 10. Effect of flow rate on breakthrough curve

TABLE-2
EXPERIMENTAL CONDITION AND RESULT OF FIXED BED REACTOR

Experimental variable	Velocity (mL/min)	H_2O concentration (ppm)	Packing amount (g)	Bed height (mm)	m_{break}/m_{max} (%)	m_{total}/m_{max} (%)	m_{total} (μmol)
Water concentration	175	10000	0.5	20	72.5	93.5	2.6
	175	6000	0.5	20	72.8	94.5	2.6
	175	3000	0.5	20	73.2	93.8	2.6
Flow rate	100	10000	0.5	20	84.6	96.6	2.6
	175	10000	0.5	20	72.4	93.5	2.6
	250	10000	0.5	20	61.1	90.7	2.6
Alloy loading mass	175	10000	0.25	10	43.6	88.7	1.3
	175	10000	0.5	20	72.8	93.5	2.6
	175	10000	0.75	30	81.8	97.4	3.9

Effect of $ZrNi_5$ loading mass: The dependence of alloy loading mass on breakthrough curve was studied by varying alloy mass from 0.25 to 0.75 g, while keeping all other operating parameters unchanged. The result is shown in Fig. 11 and Table-2, it indicates that increasing alloy loading mass caused an extension in breakthrough time, the amount of water decomposed also increased, m_{break}/m_{max} increased significantly from 43.6 to 81.8 % and m_{total}/m_{max} increased from 88.7 to 97.4 %, respectively. This result was attributed to the increase of the bed height and the gas/solid contact time at a larger sample mass. So the larger loading amount benefits to larger water decomposition amount and alloy utilization ratio.

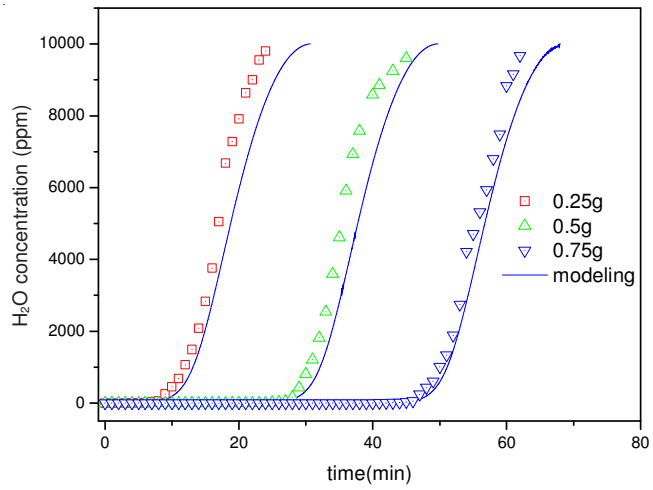

Fig. 11. Effect of $ZrNi_5$ loading amount on breakthrough curve

Model validation: The predicted breakthrough curves from mathematical modeling were shown in Figs. 9-11. It shows that all of the predicted breakthrough curves are very similar to experiment data, particularly at lower flow rate and larger alloy loading mass, the amount of water decomposed was much closer to theoretical capacity of alloy. It can be concluded that the model is able to predict the column behaviour with a good degree of accuracy.

Conclusion

In the reaction of $ZrNi_5$ powder and water vapour, Zr is the effective element to split water, transforming to ZrO_2.Ni didn't react with water and retained as element form. The reaction equation is: $ZrNi_5 + 2H_2O(g) = ZrO_2 + 5Ni + 2H_2(g)$. The reaction of $ZrNi_5$ with water could be described by first-order chemical reaction at 723 K, the kinetics equation is $G(x) = -\ln(1 - x) = k \times t$. The superficial rate constant K is proportional to water concentration. The rate equation for $ZrNi_5$ is: $\frac{dx}{dt} = K(1 - x) = k' \times c(1 - x)$, where k' is intrinsic rate constant for $ZrNi_5$ at 723 K. In fixed bed reactor, the increasing of water concentration or flow rate leads to shorter breakthrough time, the increasing of alloy loading mass results in a longer breakthrough time. The lower flow rate and higher alloy loading mass benefit to higher alloy utilization ratio and water decomposition amount much closer to theoretical value. One-dimensional quasi-homogenous model integrated with kinetics parameter could predict the fixed-bed performance. The predicted breakthrough curves agree well with experimental data.

ACKNOWLEDGEMENTS

The support from China Magnetic Confinement Nuclear Fusion Energy Special Rearch (2010GB112000) for this study is gratefully acknowledged.

REFERENCES

1. F. Ghezzi, W.T. Shmayda, N. Venkataramani and G. Bonizzoni, *Fusion Eng. Design*, **28**, 367 (1995).
2. H. Yoshida, O. Kveton, J. Koonce, D. Holland and R. Haange, *Fusion Eng. Design*, **39-40**, 875 (1998).
3. S. Fukada, Y. Toyoshima and M. Nishikawa, *Fusion Eng. Design*, **49-50**, 805 (2000).
4. S. Heinze, P. Bussiere and Th. Pelletier, *Fusion Eng. Design*, **69**, 67 (2003).
5. S. Welte, D. Demange and R. Wagner, *Fusion Eng. Design*, **86**, 2237 (2011).
6. R.S. Willms, S. Konishi and K. Okuno, *Fusion Technol.*, **26**, 659 (1994).
7. F. Ghezzi and C. Boffito,*Vacuum*, **47**, 991 (1996).
8. J.E. Klein and J.S. Holder, *Fusion Sci. Technol.*, **54**, 611 (2008).
9. S.M. Filipek, P.B. Valerie and R.S. Liu, *Appl. Surf. Sci.*, **257**, 8237 (2011).
10. D. Escobar, S. Srinivasan, Y.G. Goswami and E. Stefanakos, *J. Alloys Comp.*, **458**, 223 (2008).
11. Z. Zulfadhly, M.D. Mashitah and S. Bhatia, *Environ. Pollut.*, **112**, 463 (2001).
12. B.L. Dou, J.S. Gao, S.W. Baek and X.Z. Sha, *Energy Fuels*, **17**, 874 (2003).
13. S.H. Othman, M.A. Sohsah and M.M. Ghoneim, *Ind. Eng. Chem. Res.*, **45**, 2808 (2006).
14. T. Kawano, *Fusion Eng. Design*, **81**, 791 (2006).
15. S.K. Lee, H.S. Kim and S.J. Noh, *J. Korean Phys. Soc.*, **59**, 3019 (2011).
16. A.N. Perevezentsev, B.M. Andreev, A.N. Borisenko and A.B. Kruglov, *J. Alloys Comp.*, **335**, 246 (2002).